Eur. Phys. J. A **12**, 103–115 (2001)

THE EUROPEAN PHYSICAL JOURNAL A

Radiative decays of basic scalar, vector and tensor mesons and the determination of the P-wave $q\bar{q}$ multiplet

A.V. Anisovich, V.V. Anisovich[a], and V.A. Nikonov

Theory Division of Petersburg Nuclear Physics Institute, 188300 Gatchina, S. Petersburg district, Russia

Received: 23 August 2001 / Revised version: 13 September 2001
Communicated by Th. Walcher

Abstract. We perform simultaneous calculations of the radiative decays of scalar mesons $f_0(980) \to \gamma\gamma$, $a_0(980) \to \gamma\gamma$, vector meson $\phi(1020) \to \gamma f_0(980), \gamma a_0(980), \gamma\pi^0, \gamma\eta, \gamma\eta'$ and tensor mesons $a_2(1320) \to \gamma\gamma$, $f_2(1270) \to \gamma\gamma$, $f_2(1525) \to \gamma\gamma$, assuming all these states to be dominantly the $q\bar{q}$ ones. A good description of the considered radiative decays is reached by using almost the same radial wave functions for scalar and tensor mesons that supports the idea for the $f_0(980)$, $a_0(980)$ and $a_2(1320)$, $f_2(1270)$, $f_2(1525)$ to belong to the same P-wave $q\bar{q}$ multiplet.

PACS. 13.40.Hq Electromagnetic decays – 12.38.-t Quantum chromodynamics – 14.40.-n Mesons

1 Introduction

Despite a long history of the P-wave $q\bar{q}$ multiplet [1] the problem of definition of $q\bar{q}$ scalars is still a subject of lively discussion, see, *e.g.*, [2–4] and references therein. Radiative decays of mesons may serve as a useful tool for the study of $q\bar{q}$ structure of mesons, in particular, P-wave $q\bar{q}$ component in $f_0(980)$ and $a_0(980)$. In this way, it is rather important to investigate simultaneously the other mesons which belong to the P-wave $q\bar{q}$ multiplet, namely, tensor mesons $a_2(1320)$, $f_2(1270)$ and $f_2(1525)$. In the present paper, combined calculations of the decays $a_0(980) \to \gamma\gamma$, $f_0(980) \to \gamma\gamma$, $a_2(1320) \to \gamma\gamma$, $f_2(1270) \to \gamma\gamma$, and $f_2(1525) \to \gamma\gamma$ are carried out assuming the $q\bar{q}$ radial wave functions in these mesons to be nearly the same.

Radiative decays of the ϕ-meson are another source of important information on scalar mesons. We have calculated the decay processes with the production of mesons belonging to scalar and pseudoscalar sectors: $\phi(1020) \to \gamma f_0(980), \gamma a_0(980)$ and $\phi(1020) \to \gamma\pi_0, \gamma\eta, \gamma\eta'$. These latter, of the type of $V \to \gamma P$, are the classical reactions, which had been used rather long ago for the determination of $q\bar{q}$ structure of vector and pseudoscalar mesons [5].

We believe that simultaneous description of the processes $S \to \gamma\gamma$, $T \to \gamma\gamma$, $V \to \gamma S$ and $V \to \gamma P$ is a necessary test for the whole calculation procedure and determination of the P-wave $q\bar{q}$ multiplet.

In calculations of the decay form factors we use spectral integration over $q\bar{q}$ states together with the light-cone wave functions for the $q\bar{q}$-mesons; the method of the spectral integration for the form factor amplitudes has been developed in a set of papers [6–9].

In sect. 2 we present necessary elements of the technique for the calculation of radiative decay amplitudes. The detailed presentation of the technique for the description of composite $q\bar{q}$ systems can be found in refs. [7–9], where the pion form factor was studied together with transition form factors $\pi^0 \to \gamma(Q^2)\gamma$, $\eta \to \gamma(Q^2)\gamma$ and $\eta' \to \gamma(Q^2)\gamma$. The method of spectral integration works for the form factor amplitudes which obey the requirement of analyticity, causality and gauge invariance. The used technique allows one to introduce the composite-particle wave functions and perform calculations in terms of the light-cone variables.

It is worth noting that this calculation technique for the processes involving bound states has a broader applicability than for the $q\bar{q}$ systems only: in [6] this method got its approbation by describing the deuteron as a composite np system, then this very technique was applied to heavy mesons [10]. For the reader's convenience, in sect. 2 we recall briefly the basic points of this approach. Then we give necessary formulae for the calculation of partial widths for the decays $V \to \gamma S$, $V \to \gamma P$, $S \to \gamma\gamma$ and $T \to \gamma\gamma$.

Results of the calculation are presented in sect. 3. First, we discuss the decay $\phi(1020) \to \gamma f_0(980)$. Our calculations show that the data on branching ratio $\mathrm{BR}(\phi(980) \to \gamma f_0(980)) = (3.4 \pm 0.4^{+1.5}_{-0.5}) \cdot 10^{-4}$ [11,12] may be described assuming the $q\bar{q}$ structure of $f_0(980)$ and varying the $s\bar{s}$ and $n\bar{n} = (u\bar{u} + d\bar{d})/\sqrt{2}$ components in a broad interval. For the flavour wave function written

[a] e-mail: anisovic@thd.pnpi.spb.ru

as $\psi_{\rm flavour}[f_0(980)] = n\bar{n}\cos\varphi + s\bar{s}\sin\varphi$ the agreement with data is reached with $25^\circ \leq |\varphi| \leq 90^\circ$.

In sect. 3, we calculate also the partial widths for the decays $\phi(1020) \to \gamma\eta, \gamma\eta', \gamma\pi^0$, with the same technique as has been used for the reaction $\phi(1020) \to \gamma f_0(980)$ and with the same parametrization of the ϕ-meson wave function. The calculations demonstrate a good agreement with data as well. It should be stressed that in fact the decays $\phi(1020) \to \gamma\eta, \gamma\eta'$ are calculated without any free parameter: these decays are governed by $s\bar{s}$ components in η and η' which are well known; the wave functions of the basic pseudoscalar and vector mesons are also known, see, *e.g.* [7,8,13]. So, the calculations of the decays $\phi(1020) \to \gamma\eta, \gamma\eta'$ are needed for the verification of the method only, and the results provide us with a strong argument that the applied method for the calculation of the radiative decays of $q\bar{q}$-mesons is wholly reliable. The decay $\phi(1020) \to \gamma\pi^0$ allows us to estimate the admixture of the $n\bar{n}$ component in $\phi(1020)$. With the flavour wave function of the $\phi(1020)$ written as $\psi_{\rm flavour}(\phi(1020)) = s\bar{s}\cos\varphi_V + n\bar{n}\sin\varphi_V$, we have $|\varphi_V| \leq 4^\circ$. The partial width of $\phi(1020) \to \gamma a_0(980)$ is also proportional to the probability of the $n\bar{n}$ component in $\phi(1020)$; we discuss this decay in sect. 3 as well.

Two-photon radiative decays provide important information about P-wave $q\bar{q}$-mesons; the technique for the calculation of scalar- and tensor-meson decays, $S \to \gamma\gamma$ and $T \to \gamma\gamma$, is presented in sect. 2.

Under the assumption of the $q\bar{q}$ structure of $a_0(980)$ and $f_0(980)$, analysis of the partial widths $a_0(980) \to \gamma\gamma$ and $f_0(980) \to \gamma\gamma$ has been performed in [9]. The data for $a_0(980) \to \gamma\gamma$ are in reasonable agreement with calculation. Concerning the $f_0(980)$, the extraction of the signal $f_0(980) \to \gamma\gamma$ from the measured spectra $\gamma\gamma \to \pi\pi$ faces strong interference "resonance + background", thus resulting in uncontrollable errors (see, for example, the K-matrix calculation of the S-wave spectra $\gamma\gamma \to \pi\pi$ [14]). The recently obtained partial width $\Gamma(f_0(980) \to \gamma\gamma) = 0.28^{+0.09}_{-0.13}$ keV [15] is a factor 2 smaller than the averaged value reported previously (0.56 ± 0.11 keV [16]). In sect. 3 we re-analyse the decay $f_0(980) \to \gamma\gamma$ using new data for the width. Thus, we get two allowed intervals for the $n\bar{n}/s\bar{s}$ mixing angle: $80^\circ \leq \varphi \leq 93^\circ$ and $(-54^\circ) \leq \varphi \leq (-42^\circ)$. The restrictions for mixing angle φ which come from the combined analysis of the radiative decays $\phi(1020) \to \gamma f_0(980)$ and $f_0(980) \to \gamma\gamma$ are discussed in sect. 4; we have two solutions for φ:

$$\varphi = -48^\circ \pm 6^\circ, \qquad \varphi = 86^\circ \pm 3^\circ\,. \tag{1}$$

For positive mixing angle, the analysis gives us strong restriction for the value of the radius of $f_0(980)$: $R^2_{f_0(980)} \leq 7$ GeV^{-2} (remind that the pion radius squared is $R^2_\pi \simeq 10$ GeV^{-2}).

In sect. 3 we discuss also the results of the calculation of tensor-meson two-photon decays: $a_2(1320) \to \gamma\gamma$, $f_2(1270) \to \gamma\gamma$ and $f_2(1525) \to \gamma\gamma$. The form factors of the corresponding transitions depend strongly on the choice of the vertex $T \to q\bar{q}$. In line with the $q\bar{q}$ classification, we perform comparison with data for the vertex which is related to the dominant $q\bar{q}$ P-wave. The results are in reasonable agreement with the measured partial width $\Gamma(a_2(1320) \to \gamma\gamma)$, calculations being carried out with the wave function of $a_2(1320)$ whose characteristics are close to those of $a_0(980)$, namely, $R^2_{a_2(1320)} \simeq R^2_{a_0(980)} \simeq 7$–$12$ GeV^{-2}. Description of the two-photon decays of $f_2(1270)$ and $f_2(1525)$ fixes the $n\bar{n}/s\bar{s}$ ratio for these states. With flavour wave functions written as $\psi_{\rm flavour}[f_2(1270)] = n\bar{n}\cos\varphi_T + s\bar{s}\sin\varphi_T$ and $\psi_{\rm flavour}[f_2(1525)] = -n\bar{n}\sin\varphi_T + s\bar{s}\cos\varphi_T$, simultaneous description of the data can be reached at $R^2_{f_2(1270)} \simeq R^2_{f_2(1525)} \simeq 7$–$10$ GeV^{-2}, requiring either $\varphi_T \simeq 0^\circ$ or $\varphi_T \simeq 25^\circ$.

Simultaneous description of radiative decays of scalar and tensor mesons, $f_0(980)$, $a_0(980)$ and $a_2(1320)$, $f_2(1270)$, $f_2(1525)$, with the use of similar radial wave functions, argues in favour of their belonging to the same P-wave $q\bar{q}$ multiplet.

2 Radiative decays in the framework of the spectral integration technique

Given here are the formulae for partial widths of the radiative decays: $V \to \gamma S$, $V \to \gamma P$, $S \to \gamma\gamma$ and $T \to \gamma\gamma$. Using as an example the reaction $V \to \gamma S$, we present necessary elements of the spectral integration technique applied for the calculation of transition form factors.

2.1 Moment operators for the transition amplitudes $S \to \gamma\gamma$, $T \to \gamma\gamma$, $V \to \gamma S$ and $V \to \gamma P$

For the amplitudes under consideration, we present the moment operators for the two-photon decays of the scalar and tensor mesons: $f_0(980)$, $a_0(980) \to \gamma\gamma$ and $f_2(1270)$, $a_2(1320)$, $f_2(1525) \to \gamma\gamma$, and for the radiative decays of the ϕ-meson: $\phi(1020) \to \gamma\pi^0$, $\gamma\eta$, $\gamma\eta'$, $\gamma a_0(980)$, $\gamma f_0(980)$. Systematic presentation of the moment operators is given in [17].

2.1.1 Transition amplitude $S \to \gamma\gamma$

The transition amplitude $S \to \gamma_\perp(q^2)\gamma_\perp(q'^2)$ for the transversely polarized photons reads

$$A_{\alpha\beta} = e^2 F_{S\to\gamma\gamma}(q^2, q'^2) g^{\perp\perp}_{\alpha\beta}\,. \tag{2}$$

Here e is the electron charge ($e^2/4\pi = \alpha = 1/137$); the indices α,β refer to the photons; q and q' are the photon momenta. The metric tensor $g^{\perp\perp}_{\alpha\beta}$ works in the space orthogonal to $p = q + q'$ and q:

$$g^{\perp\perp}_{\alpha\beta} = g_{\alpha\beta} - \frac{q_{\perp\alpha}q_{\perp\beta}}{q^2_\perp} - \frac{p_\alpha p_\beta}{p^2}\,,$$
$$q_{\perp\alpha} = g^\perp_{\alpha\alpha'}q_{\alpha'}\,, \qquad g^\perp_{\alpha\alpha'} = g_{\alpha\alpha'} - \frac{p_\alpha p_{\alpha'}}{p^2}\,. \tag{3}$$

2.1.2 Tensor meson decay amplitude $T \to \gamma\gamma$

The $T \to \gamma\gamma$ decay amplitude has the following structure:

$$A_{\mu\nu,\alpha\beta} = e^2 \Big[S^{(0)}_{\mu\nu,\alpha\beta}(p,q)\; F^{(0)}_{T\to\gamma\gamma}(0,0) + S^{(2)}_{\mu\nu,\alpha\beta}(p,q)\; F^{(2)}_{T\to\gamma\gamma}(0,0) \Big] , \quad (4)$$

where $S^{(0)}_{\mu\nu,\alpha\beta}(p,q)$ and $S^{(2)}_{\mu\nu,\alpha\beta}(p,q)$ are the moment operators, indices α,β refer to photons and μ,ν to the tensor meson. Two transition form factors for the transversely polarized photons $T \to \gamma_\perp(q^2)\gamma_\perp(q'^2)$, namely, $F^{(0)}_{T\to\gamma\gamma}(q^2,q'^2)$ and $F^{(2)}_{T\to\gamma\gamma}(q^2,q'^2)$, depend on the photon momenta squared q^2 and q'^2; the limit $q^2 = q'^2 = 0$ corresponds to the two-photon decay.

The moment operators read

$$S^{(0)}_{\mu\nu,\alpha\beta}(p,q) = \left(\frac{q_{\perp\mu} q_{\perp\nu}}{q^2_\perp} - \frac{1}{3} g^\perp_{\mu\nu} \right) g^{\perp\perp}_{\alpha\beta} \quad (5)$$

and

$$S^{(2)}_{\mu\nu\,,\,\alpha\beta}(p,q) = g^{\perp\perp}_{\mu\alpha} g^{\perp\perp}_{\nu\beta} + g^{\perp\perp}_{\mu\beta} g^{\perp\perp}_{\nu\alpha} - g^{\perp\perp}_{\mu\nu} g^{\perp\perp}_{\alpha\beta} \; . \quad (6)$$

The moment operators are orthogonal in the space of photon polarizations: $S^{(0)}_{\mu\nu,\alpha\beta} S^{(2)}_{\mu'\nu',\alpha\beta} = 0$.

2.1.3 Transition amplitude $V \to \gamma S$

The transition amplitude $V \to \gamma_\perp(q^2) S$ for the transversely polarized photon takes the form

$$A_{\mu\alpha} = e F_{V\to\gamma S}(q^2) g^{\perp\perp}_{\mu\alpha} \; . \quad (7)$$

The index α refers to the photon and μ to the vector meson; p and q are the momenta of the initial vector meson and photon. The metric tensor $g^{\perp\perp}_{\mu\alpha}$ works in the space orthogonal to p and q. The limit $q^2 = 0$ corresponds to the radiative decay of the vector meson.

2.1.4 Transition amplitude $V \to \gamma P$

The spin operator for the amplitude $V \to \gamma P$ contains the antisymmetric tensor $\epsilon_{\mu\nu\alpha\beta}$, and the amplitude has the following structure:

$$A_{\mu\alpha} = e\, \epsilon_{\mu\alpha\nu_1\nu_2} p_{\nu_1} q_{\nu_2} F_{V\to\gamma P}(q^2) \; . \quad (8)$$

The notations are the same as for $V \to \gamma S$.

2.2 Form factor for the radiative decay $V \to \gamma_\perp(q^2)S$

The method of calculation of the three-point form factor amplitudes in terms of the spectral representations over the $q\bar{q}$ intermediate-state masses was developed in [7]. Here we give a schematic presentation of the method using the reaction $V \to \gamma_\perp(q^2)S$ as an example.

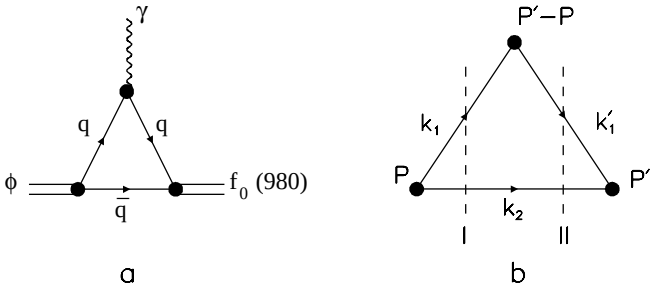

Fig. 1. a) Diagrammatic representation of the transition $\phi(1020) \to \gamma f_0(980)$. b) Three-point quark diagram: dashed lines I and II mark two cuttings in the double spectral representation.

2.2.1 Double spectral representation of the form factor

Assuming the $q\bar{q}$ structure for the initial (V) and final (S) mesons, the amplitude of the decay $V \to \gamma S$ is determined by the subprocesses $V \to q\bar{q}$ and $q\bar{q} \to S$, with the emission of $\gamma(q^2)$, see fig. 1a. The corresponding three-point loop diagram is calculated using a double spectral representation over intermediate $q\bar{q}$ states: they are marked by dashed lines in fig. 1b.

To be illustrative, let us start with the three-point Feynman diagram. For the process of fig. 1a one has

$$A^{(\mathrm{Feynman})}_{\mu\nu} = \int \frac{\mathrm{d}^4 k}{i(2\pi)^4}\, G_V \times \frac{Z^{(q\bar{q})}_{V\to\gamma S}\, S^{(V\to\gamma S)}_{\mu\nu}}{(m^2 - k_1^2)(m^2 - k_1'^2)(m^2 - k_2^2)}\, G_S \, . \quad (9)$$

Here k_1, k_1', k_2 are the quark momenta, m is the quark mass, and G_V, G_S are quark-meson vertices; the quark charges are included into $Z^{(q\bar{q})}_{V\to\gamma S}$. The spin-dependent block reads

$$S^{(V\to\gamma S)}_{\mu\nu} = -\mathrm{Sp}\left[(\hat{k}_1' + m) \gamma^\perp_\mu (\hat{k}_1 + m) \gamma^\perp_\nu (-\hat{k}_2 + m) \right] , \quad (10)$$

where the Dirac matrices $\gamma^\perp_\mu$ and $\gamma^\perp_\nu$ are orthogonal to the emitted momenta: $\gamma^\perp_\mu q_\mu = 0$ and $\gamma^\perp_\nu p_\nu = 0$.

To transform the Feynman integral (9) into double spectral integral over invariant $q\bar{q}$ masses squared, one should make the following steps:
i) consider the corresponding energy-off-shell diagram, fig. 1b, with $P^2 = (k_1 + k_2)^2 \geq 4m^2$, $P'^2 = (k_1' + k_2)^2 \geq 4m^2$ and fixed momentum transfer squared $q^2 = (P - P')^2$,
ii) extract the invariant amplitude by separating spin operators,
iii) calculate the discontinuities of the invariant amplitude over intermediate $q\bar{q}$ states marked in fig. 1b by dashed lines.

The double discontinuity is the integrand of the spectral integral over P^2 and P'^2. Furthermore, we put the following notations:

$$P^2 = s, \qquad P'^2 = s' \, . \quad (11)$$

For the calculation of discontinuity, by cutting the Feynman diagram, the pole terms of the propagators are replaced with their residues: $(m^2-k^2)^{-1} \to \delta(m^2-k^2)$. So, the particles in the intermediate states marked by dashed lines I and II in fig. 1b are mass-on-shell, $k_1^2 = k_2^2 = k_1'^2 = m^2$. As a result, the Feynman diagram integration turns into the integration over phase spaces of the cut states. The corresponding phase space for the three-point diagram reads

$$\begin{aligned}&\mathrm{d}\Phi(P,P';k_1,k_2,k_1') = \\ &\mathrm{d}\Phi(P;k_1,k_2)\mathrm{d}\Phi(P';k_1',k_2')(2\pi)^3 2k_{20}\delta^{(3)}(\mathbf{k}_2'-\mathbf{k}_2)\,, \quad (12)\end{aligned}$$

where the invariant two-particle phase space $\mathrm{d}\Phi(P;k_1,k_2)$ is determined as follows:

$$\begin{aligned}&\mathrm{d}\Phi(P;k_1,k_2) = \\ &\frac{1}{2}\frac{\mathrm{d}^3k_1}{(2\pi)^3 2k_{10}}\frac{\mathrm{d}^3k_2}{(2\pi)^3 2k_{20}}(2\pi)^4\delta^{(4)}(P-k_1-k_2)\,. \quad (13)\end{aligned}$$

The last step is to single out the invariant component from the spin factor (10). According to (7), the spin factor (10) is proportional to the metric tensor, $S_{\mu\nu}^{(V\to\gamma S)} \sim g_{\mu\nu}^{\perp\perp}$, which works in the space of the intermediate-state momenta. Then the spin factor $S_{V\to\gamma S}^{\mathrm{tr}}$, determined as

$$S_{\mu\nu}^{(V\to S)} = g_{\mu\nu}^{\perp\perp} S_{V\to\gamma S}(s,s',q^2), \quad (14)$$

is equal to

$$\begin{aligned}&S_{V\to\gamma S}(s,s',q^2) = \\ &-2m\left(4m^2+s-s'+q^2-\frac{4ss'\alpha(s,s',q^2)}{s+s'-q^2}\right), \quad (15)\end{aligned}$$

$$\alpha(s,s',q^2) = \frac{q^2(s+s'-q^2)}{2q^2(s+s')-(s-s')^2-q^4}\,.$$

Recall that, when going from (10) to (15), we use the mass-on-shell relations $(k_1k_2) = s/2-m^2$, $(k_1'k_2) = s'/2-m^2$, and $(k_1'k_1) = m^2-q^2/2$.

The spectral integration is carried out over the energy squared of quarks in the intermediate states, $s = P^2 = (k_1+k_2)^2$ and $s' = P'^2 = (k_1'+k_2)^2$, at fixed $q^2 = (P'-P)^2$. The spectral representation for the amplitude $A_{V\to\gamma S}(q^2)$ reads

$$\begin{aligned}A_{V\to\gamma S}(q^2) &= \int\limits_{4m^2}^{\infty}\frac{\mathrm{d}s}{\pi}\int\limits_{4m^2}^{\infty}\frac{\mathrm{d}s'}{\pi}\frac{G_V(s)}{s-M_V^2}\frac{G_S(s')}{s'-M_S^2} \\ &\times\int \mathrm{d}\Phi(P,P';k_1,k_2),k_1'\,S_{V\to\gamma S}^{(\mathrm{tr})}(s,s',q^2)Z_{V\to\gamma S}^{(q\bar{q})}\,. \quad (16)\end{aligned}$$

The spectral representation of the amplitude $A_{V\to\gamma S}(q^2)$ gives us the invariant part of $A_{\mu\nu}^{(\mathrm{Feynman})}$, eq. (9), when the vertices, $G_V(s)$ and $G_S(s')$, are constant. Generally, the energy-dependent vertices can be incorporated into spectral integrals. According to [6], the form factor of a composite system can be obtained by considering the two-particle partial-wave scattering amplitude $1+2 \to 1+2$: the pole sigularity of this amplitude corresponds to the composite system. The amplitude for the emission of a photon by the two-particle-interaction system has two poles related to the states "before" and "after" electromagnetic interaction, and the two-pole residue of this amplitude provides us the form factor of the composite system. When a partial-wave scattering amplitude is treated using the dispersion relation N/D-method, the vertex $G(s)$ is determined by the N-function: the vertex as well as the N-function have left-hand side singularities which are determined by forces between the particles 1 and 2.

It is reasonable to name the ratios $G_V(s)/(s-m^2)$ and $G_S(s')/(s'-m^2)$ the wave functions of vector and scalar particle, respectively:

$$\frac{G_V(s)}{s-m^2} = \psi_V(s)\,, \qquad \frac{G_S(s')}{s'-m^2} = \psi_S(s')\,. \quad (17)$$

Working with eq. (16), one can express it in terms of the light-cone variables.

2.2.2 Light-cone variables

One can transform eq. (16) to the light-cone variables, using the boost along the z-axis. Let us use the frame where the initial vector meson moves along the z-axis with the momentum $p \to \infty$:

$$P = (p+\frac{s}{2p},\mathbf{0},p), \qquad P' = (p+\frac{s'+q_\perp^2}{2p},-\mathbf{q}_\perp,p). \quad (18)$$

In this frame the two-particle phase space is equal to

$$\begin{aligned}&\mathrm{d}\Phi(P;k_1,k_2) = \\ &\frac{1}{16\pi^2}\frac{\mathrm{d}x_1\mathrm{d}x_2}{x_1x_2}\mathrm{d}^2k_{1\perp}\mathrm{d}^2k_{2\perp}\delta(1-x_1-x_2)\delta^{(2)}(\mathbf{k}_{1\perp}+\mathbf{k}_{2\perp}) \\ &\times\delta\left(s-\frac{m^2+k_{1\perp}^2}{x_1}-\frac{m^2+k_{2\perp}^2}{x_2}\right), \quad (19)\end{aligned}$$

where $x_i = k_{iz}/p$, and the phase space for the triangle diagram reads

$$\begin{aligned}&\mathrm{d}\Phi(P,P';k_1,k_2,k_1') = \\ &\frac{1}{16\pi}\frac{\mathrm{d}x_1\mathrm{d}x_2}{x_1^2x_2}\mathrm{d}^2k_{1\perp}\mathrm{d}^2k_{2\perp}\delta(1-x_1-x_2)\delta^{(2)}(\mathbf{k}_{1\perp}+\mathbf{k}_{2\perp})\,, \\ &\delta\left(s-\frac{m^2+k_{1\perp}^2}{x_1}-\frac{m^2+k_{2\perp}^2}{x_2}\right) \\ &\times\ \delta\left(s'+q_\perp^2-\frac{m^2+(\mathbf{k}_{1\perp}-\mathbf{q}_\perp)^2}{x_1}-\frac{m^2+k_{2\perp}^2}{x_2}\right). \quad (20)\end{aligned}$$

Then the amplitude $V \to \gamma(q^2)S$ is written as

$$\begin{aligned}A_{V\to\gamma(q^2)S}(q^2) &= \frac{Z_{V\to\gamma S}^{(q\bar{q})}}{16\pi^3}\int\limits_0^1\frac{\mathrm{d}x}{x(1-x)^2} \\ &\times\int \mathrm{d}^2k_\perp\psi_V(s)\psi_S(s')S_{V\to\gamma S}(s,s',q^2)\,, \quad (21)\end{aligned}$$

where $x = k_{2z}/p$, $\mathbf{k}_\perp = \mathbf{k}_{2\perp}$, and the $q\bar{q}$ invariant-masses squared are

$$s = \frac{m^2 + k_\perp^2}{x(1-x)}\,, \qquad s' = \frac{m^2 + (\mathbf{k}_\perp + x\mathbf{q}_\perp)^2}{x(1-x)}\,. \qquad (22)$$

2.2.3 Charge factors

Charge factors for the $n\bar{n}$ and $s\bar{s}$ components in the transition $\phi \to \gamma f_0$ are determined as

$$Z^{(n\bar{n})}_{\phi\to\gamma f_0} = 2\zeta^{(n\bar{n})}_{\phi\to\gamma f_0} = \frac{1}{6}\,, \qquad (23)$$

$$Z^{(s\bar{s})}_{\phi\to\gamma f_0} = 2\zeta^{(s\bar{s})}_{\phi\to\gamma f_0} = 2e_s = -\frac{2}{3}\,,$$

where $\zeta^{(n\bar{n})}_{\phi\to\gamma f_0}$ is the following convolution: $\zeta^{(n\bar{n})}_{\phi\to\gamma f_0} = (u\bar{u}+d\bar{d})/\sqrt{2}\cdot\hat{e}_q\cdot(u\bar{u}+d\bar{d})/\sqrt{2} = (e_u+e_d)/2$. Here e_u and e_d are charges of u and d quarks. The factor 2 in (23) is related to two possibilities for photon emission, namely, from quark and antiquark. Likewise, for the process $\phi \to \gamma a_0$, one has

$$Z_{\phi\to\gamma a_0} = 2\zeta_{\phi\to\gamma a_0} = e_u - e_d = 1\,. \qquad (24)$$

2.2.4 Meson wave functions

To calculate the form factors, one should define meson wave functions. Following [18], we parametrize the wave functions in the exponential form:

$$\psi_V(s) = C_V e^{-b_V s}, \qquad \psi_S(s) = C_S e^{-b_S s}\,. \qquad (25)$$

The parameters b_V and b_S characterize the size of the system, they are related to the mean radii squared, R_V^2 and R_S^2, of the mesons. At fixed R_V^2 and R_S^2 the constants C_V and C_S are determined by the wave function normalization, which itself is given by the meson form factor in the external field, $F_{\rm meson}(q^2)$, and at small q^2 the form factor is

$$F_{\rm meson}(q^2) \simeq 1 + \frac{1}{6}R^2_{\rm meson}q^2\,. \qquad (26)$$

The requirement $F_{\rm meson}(0) = 1$ fixes the constant $C_{\rm meson}$ in (25), while the value $R^2_{\rm meson}$ is directly related to $b_{\rm meson}$.

In terms of the light-cone variables, the form factor $F_{\rm meson}(q^2)$ reads

$$F_{\rm meson}(q^2) = \frac{1}{16\pi^3}\int\limits_0^1 \frac{{\rm d}x}{x(1-x)^2}$$
$$\times \int {\rm d}^2k_\perp \Psi_{\rm meson}(s)\Psi_{\rm meson}(s')S^{\rm (tr)}_{\rm meson}(s,s',q^2)\,, \qquad (27)$$

where $S^{\rm (tr)}_{\rm meson}$ is determined by the following traces:

$$2P^\perp_\mu S^{\rm (tr)}_S(s,s',q^2) =$$
$$-{\rm Sp}\left[(\hat{k}'_1+m)\gamma^\perp_\mu(\hat{k}_1+m)(-\hat{k}_2+m)\right]\,,$$

$$2P^\perp_\mu S^{\rm (tr)}_V(s,s',q^2) =$$
$$-\frac{1}{3}{\rm Sp}\left[\gamma'^\perp_\alpha(\hat{k}'_1+m)\gamma^\perp_\mu(\hat{k}_1+m)\gamma^\perp_\alpha(-\hat{k}_2+m)\right] \qquad (28)$$

and the orthogonal components entering (28) are as follows:

$$P^\perp_\mu = P_\mu - q_\mu\frac{(Pq)}{q^2}\,, \qquad \gamma^\perp_\mu = \gamma_\mu - q_\mu\frac{\hat{q}}{q^2}\,,$$
$$\gamma^\perp_\alpha = \gamma_\alpha - P_\alpha\frac{\hat{P}}{P^2}\,, \qquad \gamma'^\perp_\alpha = \gamma_\alpha - P'_\alpha\frac{\hat{P}'}{P'^2}\,, \qquad (29)$$

where $q = k'_1 - k_1$. When determining $S^{\rm (tr)}_V(s,s',q^2)$, we have averaged over three polarizations of the vector meson that results in the factor 1/3.

The functions $S^{\rm (tr)}_S(s,s',q^2)$ and $S^{\rm (tr)}_V(s,s',q^2)$ are equal to

$$S^{\rm (tr)}_S(s,s',q^2) = \alpha(s,s',q^2)(s+s'-8m^2-q^2)+q^2\,,$$
$$S^{\rm (tr)}_V(s,s',q^2) = \frac{2}{3}\left[\alpha(s,s',q^2)(s+s'+4m^2-q^2)+q^2\right], \qquad (30)$$

where $\alpha(s,s',q^2)$ is given in (15).

The problem of the calculation accuracy by using the exponential type of wave functions was investigated in [18], where two calculation variants had been carried out as follows:
1) with the wave functions for η- and η'-mesons reconstructed by using the reactions $\eta \to \gamma(Q^2)\gamma$ and $\eta' \to \gamma(Q^2)\gamma$ at Q^2 being varied in a broad interval,
2) with exponential-type parametrization of wave functions.

Both calculation variants provided us with results which are close to each other at the same values of R^2_η and $R^2_{\eta'}$; the difference is about 2% for the decay form factors.

2.2.5 Partial width

The decay partial width is determined as

$$m_V\Gamma_{V\to\gamma S} = \frac{1}{3}\int {\rm d}\Phi(p_V;q,p'_S)|A_{\mu\nu}|^2\,. \qquad (31)$$

Here averaging over spin projections of the ϕ-meson and summing over photon ones is carried out (summation over photon spin variables results in the metric tensor $g^{\perp\perp}_{\mu\mu'}$); the two-particle phase space for the radiative decay $V \to \gamma + S$ is equal to $\int {\rm d}\,\Phi(p_V;q,p'_S) = (m_V^2 - m_S^2)/(16\pi m_V^2)$. The partial width in terms of the form factor reads

$$m_V\Gamma_{V\to\gamma S} = \frac{1}{6}\alpha\frac{m_V^2 - m_S^2}{m_V^2}|F_{V\to\gamma S}(0)|^2\,. \qquad (32)$$

2.3 The process V → γP

The light-cone representation of the transition form factor $V \to \gamma_\perp(q^2)P$ reads

$$F_{V\to\gamma P}(q^2) = \frac{Z_{V\to\gamma P}}{16\pi^3}\int\limits_0^1 \frac{{\rm d}x}{x(1-x)^2}$$
$$\times \int {\rm d}^2k_\perp \Psi_V(s)\Psi_P(s')S_{V\to\gamma P}(s,s',q^2), \qquad (33)$$

The spin factor for pseudoscalar mesons is determined by

$$-\mathrm{Sp}\left[i\gamma_5(\hat{k}_1'+m)\gamma_\alpha^{\perp\perp}(\hat{k}_1+m)\gamma_\mu'^{\perp}(-\hat{k}_2+m)\right] = \epsilon_{\mu\alpha\nu_1\nu_2}P_{\nu_1}\tilde{q}_{\nu_2}S_{V\to\gamma P}(s,s',q^2) \quad (34)$$

where $\tilde{q}=P-P'$ and $\tilde{q}_\alpha\gamma_\alpha^{\perp\perp}=0$, $P'_\mu\gamma_\mu'^{\perp}=0$. The spin factor is equal to

$$S_{V\to\gamma P}(s,s',q^2)=4m\,. \quad (35)$$

Charge factors for the considered radiative decays are as follows: for the $s\bar{s}$ component in the reactions $\phi\to\gamma\eta,\gamma\eta'$, $Z^{(s\bar{s})}_{\phi\to\gamma\eta}=Z^{(s\bar{s})}_{\phi\to\gamma\eta'}=-2/3$, and for the π^0 and $a_0(980)$ productions, $Z_{\phi\to\gamma\pi^0}=Z_{\phi\to\gamma a_0(980)}=1$.

The partial width for the decay $V\to\gamma P$ is equal to

$$m_V\Gamma_{V\to\gamma P}=\frac{1}{3}\int \mathrm{d}\Phi(p_V;q,p'_P)|A_{\mu\nu}|^2 = \frac{1}{6}\alpha\frac{m_V^2-m_P^2}{m_V^2}|F_{V\to\gamma P}(0)|^2\,. \quad (36)$$

2.4 Processes S → γγ

Our calculation of the two-photon decays of scalar and tensor mesons is based on the method developed in [8] for the study of the pseudoscalar meson transitions $\pi^0\to\gamma(q^2)\gamma$, $\eta\to\gamma(q^2)\gamma$ and $\eta'\to\gamma(q^2)\gamma$; and for the photon we use the quark-antiquark wave function which was found in [8]. We perform the calculation of the scalar- and tensor-meson transition form factors $S\to\gamma(q^2)\gamma$ and $T\to\gamma(q^2)\gamma$ in the region of small q^2; these form factors, in the limit $q^2\to 0$, determine the partial widths $S\to\gamma\gamma$ and $T\to\gamma\gamma$.

The transition form factor $q\bar{q}$-meson $\to\gamma(q^2)\gamma$ is determined by the three-point quark loop diagram of the type of fig. 1b that is a convolution of the $q\bar{q}$-meson and photon wave functions, $\psi_{q\bar{q}}\otimes\psi_\gamma$. Following [8], we represent the photon wave function as a sum of two components which describe the prompt production of the $q\bar{q}$ pair in the large s' (with a point-like vertex for the transition $\gamma\to q\bar{q}$) as well as in the low-s' region where the vertex $\gamma\to q\bar{q}$ has a nontrivial structure due to soft $q\bar{q}$ interactions. The process of fig. 1b at moderately small $|q^2|$ is mainly saturated by the contribution of the low-s' region, in other words, by the soft component of the photon wave function. The soft component of the photon wave function was restored in [8] on the basis of experimental data for the transition $\pi^0\to\gamma(q^2)\gamma$ at $|q^2|\le 1$ GeV^2; it is shown in fig. 2.

Once the photon wave function is found, the decay form factors $S\to\gamma\gamma$ and $T\to\gamma\gamma$ provide the opportunity to investigate the scalar and tensor meson wave functions.

2.4.1 Form factor $S\to\gamma(q^2)\gamma$

Following the prescription given in the previous sections for $V\to\gamma(q^2)S$ and $V\to\gamma(q^2)P$, we present the amplitude of the process $S\to\gamma(q^2)\gamma$ in terms of the light-cone variables. The transition form factor $S\to\gamma(q^2)\gamma$ reads

$$F_{S\to\gamma\gamma}(q^2,0)=\frac{Z_{S\to\gamma\gamma}\sqrt{N_c}}{16\pi^3}\int_0^1\frac{\mathrm{d}x}{x(1-x)^2} \times\int \mathrm{d}^2k_\perp\psi_S(s)\psi_\gamma(s')S_{S\to\gamma\gamma}(s,s',q^2). \quad (37)$$

Here, as before in eq. (21), the light-cone variables are introduced as follows: $x=k_{2z}/p$, $\mathbf{k}_\perp=\mathbf{k}_{2\perp}$, and the $q\bar{q}$ invariant-masses squared, s and s', are determined by eq. (22). The factor $\sqrt{N_c}$, where $N_c=3$ is the number of colours, is related to the normalization of the photon wave function performed in [8].

The charge factor $Z_{S\to\gamma\gamma}=2\zeta_{S\to\gamma\gamma}$ is determined by the quark content of the S-meson. We have two loop diagrams with quark lines drawn clockwise and anticlockwise: the factor 2 in the determination of $Z_{S\to\gamma\gamma}$ stands for this doubling. For the f_0-meson, one has two components with different charge factors $\zeta_{n\bar{n}\to\gamma\gamma}=(e_u^2+e_d^2)/\sqrt{2}$ and $\zeta_{s\bar{s}\to\gamma\gamma}=e_s^2$, while for the a_0-meson $\zeta_{a_0\to\gamma\gamma}=(e_u^2-e_d^2)/\sqrt{2}$.

The spin structure factor $S_{S\to\gamma\gamma}(s,s',q^2)$ is fixed by the three-point quark loop trace for the amplitude of fig. 1b, with transverse polarized photons:

$$-\mathrm{Sp}[\gamma_\beta^{\perp\perp}(\hat{k}_1'+m)\gamma_\alpha^{\perp\perp}(\hat{k}_1+m)(-\hat{k}_2+m)] = S_{S\to\gamma\gamma}(s,s',q^2)\;g_{\alpha\beta}^{\perp\perp}\,. \quad (38)$$

Here $\gamma_\beta^{\perp\perp}$ and $\gamma_\alpha^{\perp\perp}$ stand for photon vertices, $\gamma_\alpha^{\perp\perp}=g_{\alpha\mu}^{\perp\perp}\gamma_\mu$, while $g_{\alpha\mu}^{\perp\perp}$ is determined by formula (3) with the following substitutions: $q\to P-P'$ and $q'\to P'$.

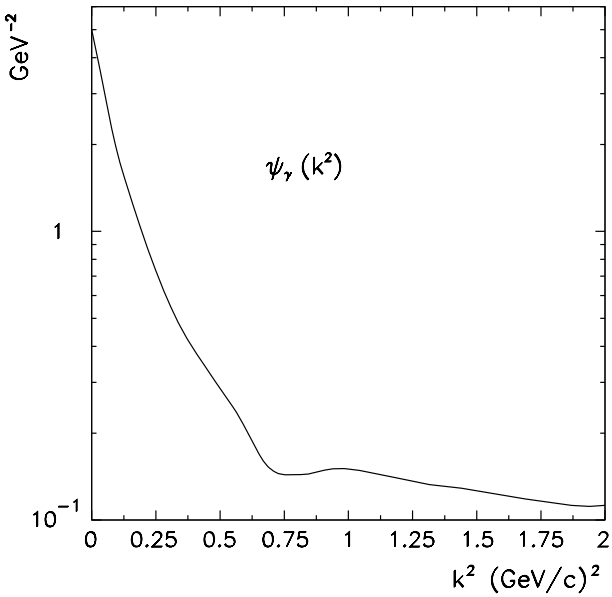

Fig. 2. Photon wave function for nonstrange quarks, $\psi_{\gamma\to n\bar{n}}(k^2)=g_\gamma(k^2)/(k^2+m^2)$, where $k^2=s/4-m^2$; the wave function for the $s\bar{s}$ component is equal to $\psi_{\gamma\to s\bar{s}}(k^2)=g_\gamma(k^2)/(k^2+m_s^2)$; the constituent quark masses are $m=350$ MeV and $m_s=500$ MeV.

One has

$$S_{S\to\gamma\gamma}(s,s',q^2) = \\ -2m\left[4m^2-s+s'+q^2-\frac{4ss'q^2}{2(s+s')q^2-(s-s')^2-q^4}\right]. \quad (39)$$

The partial width, $\Gamma_{S\to\gamma\gamma}$, is determined as follows:

$$m_S\Gamma_{S\to\gamma\gamma} = \frac{1}{2}\int \mathrm{d}\Phi(p_S;q,q')|A_{\mu\nu}|^2 = \\ \pi\alpha^2|F_{S\to\gamma\gamma}(0,0)|^2\,. \quad (40)$$

Here m_S is the scalar-meson mass, the summation is carried out over outgoing photon polarizations, the photon identity factor, 1/2, is written explicitly, and the two-photon invariant phase space is equal to $\mathrm{d}\Phi_2(p_S;q,q') = 1/(16\pi)$.

2.5 Two-photon tensor-meson decay T → γγ

The decay amplitude $T \to \gamma_\perp(q^2)\gamma$ can be considered quite analogousy to the amplitude of the two-photon scalar-meson decay. The light-cone representation for the form factor $F^{(H)}_{T\to\gamma\gamma}(q^2,q'^2=0)$ with $H=0,2$ reads

$$F^{(H)}_{T\to\gamma\gamma}(q^2,0) = \frac{Z_{T\to\gamma\gamma}\sqrt{N_c}}{16\pi^3}\int\limits_0^1 \frac{\mathrm{d}x}{x(1-x)^2} \\ \times\int \mathrm{d}^2k_\perp \psi_T(s)\psi_\gamma(s')S^{(H)}_{T\to\gamma\gamma}(s,s',q^2). \quad (41)$$

Here we use the same notation as in (37); the charge factors for the tensor and scalar mesons are equal to one another, $Z_{T\to\gamma\gamma} = Z_{S\to\gamma\gamma}$.

The spin structure factors are fixed by the vertex for transition $T \to q\bar{q}$; we denote this vertex as $T_{\mu\nu}$. One has

$$S^{(T)}_{\mu\nu,\alpha\beta} = \mathrm{Sp}[\gamma^{\perp\perp}_\beta(\hat{k}'_1+m)\gamma^{\perp\perp}_\alpha(\hat{k}_1+m)T_{\mu\nu}(\hat{k}_2-m)] = \\ S^{(0)}_{\mu\nu,\alpha\beta}(P,\tilde{q})S^{(0)}(P^2,P'^2,\tilde{q}^2) \\ +S^{(2)}_{\mu\nu,\alpha\beta}(P,\tilde{q})S^{(2)}(P^2,P'^2,\tilde{q}^2), \quad (42)$$

where $\gamma^{\perp\perp}_\alpha$ and $\gamma^{\perp\perp}_\beta$ stand for photon vertices, $\gamma^{\perp\perp}_\alpha = g^{\perp\perp}_{\alpha\alpha'}\gamma_{\alpha'}$, and $g^{\perp\perp}_{\alpha\alpha'}$ is determined by eq. (3) with the following substitutions: $q \to P-P'$ and $q' \to P'$. The moment operators $S^{(0)}_{\mu\nu,\alpha\beta}(P,\tilde{q})$ and $S^{(2)}_{\mu\nu,\alpha\beta}(P,\tilde{q})$ work also in the intermediate-state momentum space. Recall that $\tilde{q} = P-P'$ and $P^2 = s$, $P'^2 = s'$, $\tilde{q}^2 = q^2$, while the momenta k'_1, k_1 and k_2 are mass-on-shell.

The vertex $T_{\mu\nu}(k)$ in its minimal form reads

$$T_{\mu\nu}(k) = k_\mu\gamma_\nu + k_\nu\gamma_\mu - \frac{2}{3}g^\perp_{\mu\nu}\hat{k}\,, \quad (43)$$

where $k = k_1 - k_2$ and $g^\perp_{\mu\nu}P_\nu = 0$.

Spin structure factors $S^{(0)}(s,s',q^2)$ and $S^{(2)}(s,s',q^2)$ are calculated by projecting (42) on the moment operators $S^{(H)}_{\mu\nu,\alpha\beta}(P,\tilde{q})$:

$$S^{(H)}(s,s',q^2) = \frac{S^{(H)}_{\mu\nu,\alpha\beta}(P,\tilde{q})S^{(T)}_{\mu\nu,\alpha\beta}}{\left(S^{(H)}_{\mu'\nu',\alpha'\beta'}(P,\tilde{q})\right)^2}\,. \quad (44)$$

Explicit expressions for the spin structure factors $S^{(0)}(s,s',q^2)$ and $S^{(2)}(s,s',q^2)$ are rather cumbersome, and we do not present them here.

The $q\bar{q}$ (2^{++}) state can be constructed in two ways, namely, with the $q\bar{q}$ orbital momenta $L=1$ and $L=3$ (the ${}^3P_2q\bar{q}$ and ${}^3F_2q\bar{q}$ states). The vertex $T_{\mu\nu}$ of eq. (43), corresponding to the dominant P-wave $q\bar{q}$ state, includes also a certain admixture of the F-wave $q\bar{q}$ state.

The vertex for the production of pure $q\bar{q}$ $(L=1)$ state reads

$$T^{(L=1)}_{\mu\nu} = k_\mu\Gamma_\nu + k_\nu\Gamma_\mu - \frac{2}{3}g^\perp_{\mu\nu}(\Gamma k)\,, \\ \Gamma_\mu = \gamma^\perp_\mu - \frac{k_\mu}{2m+\sqrt{s}}\,, \quad (45)$$

where the operator Γ_μ selects the spin-1 state for the $q\bar{q}$ (see [6,17] for detail).

The $(L=3)$-operator for the ${}^3F_2q\bar{q}$ state is equal to

$$T^{(L=3)}_{\mu\nu} = k_\mu k_\nu(\Gamma k) - \frac{k^2}{5}\left(g^\perp_{\mu\nu}(\Gamma k)+\Gamma_\mu k_\nu+\Gamma_\nu k_\mu\right). \quad (46)$$

For the $q\bar{q}$ wave function of tensor mesons, we use a parametrization similar to that for scalar mesons, see eq. (25). The parameters C_T and b_T are determined by the tensor-meson charge form factor at small q^2, eq. (26): the charge form factor is given by eq. (27). The spin factor for the tensor meson, $S_T(s,s',q^2)$ is defined by the quark loop trace as follows:

$$\frac{1}{5}\mathrm{Sp}[T_{\mu\nu}(\hat{k}_1+m)\gamma_\alpha(\hat{k}'_1+m)T'_{\mu\nu}(\hat{k}_2-m)] = \\ 2P_{\perp\alpha}S_T(s,s',q^2), \quad (47)$$

The operator $T_{\mu\nu}$ is written for the initial state transition $T \to q\bar{q}$, eq. (43), while $T'_{\mu\nu}$ describes the production of the outgoing tensor meson $q\bar{q} \to T$ that requires the following substitutions in (43): $k_1 \to k'_1$ and $P \to P'$. The tensor meson charge form factor is averaged over polarizations that results in the factor 1/5 in (47).

The partial width, $\Gamma_{T\to\gamma\gamma}$, is determined as

$$m_T\Gamma_{T\to\gamma\gamma} = \frac{1}{2}\int \mathrm{d}\Phi(p_T;q,q')\frac{1}{5}\sum_{\mu\nu,\alpha\beta}|A_{\mu\nu,\alpha\beta}|^2 = \\ \frac{4}{5}\pi\alpha^2\left[\frac{1}{3}|F^{(0)}_{T\to\gamma\gamma}(0,0)|^2 + |F^{(2)}_{T\to\gamma\gamma}(0,0)|^2\right]. \quad (48)$$

Here m_T is the tensor-meson mass, the summation is carried out over outgoing photon polarizations, the photon identity factor, 1/2, is written explicitly; the averaging over tensor-meson polarizations results in the factor 1/5.

3 Results

In this section we present the results of the calculations of the partial widths for the radiative decays $\phi(1020) \to \gamma f_0(980)$, $\phi(1020) \to \gamma\eta, \gamma\eta', \gamma\pi^0, \gamma a_0(980)$ and two-photon decays $f_0(980) \to \gamma\gamma$, $a_0(980) \to \gamma\gamma$, $a_2(1320) \to \gamma\gamma$, $f_2(1270) \to \gamma\gamma$, $f_2(1525) \to \gamma\gamma$.

3.1 $\phi(1020) \to \gamma f_0(980)$: the decay amplitude and partial width

Here we calculate the branching ratio for the decay $\phi(1020) \to \gamma f_0(980)$ assuming the $q\bar{q}$ structure of $f_0(980)$.

3.1.1 Wave functions of $\phi(1020)$ and $f_0(980)$

We write the wave functions of $\phi(1020)$ and $f_0(980)$ as follows:

$$\Psi_\phi(s) = (n\bar{n}\sin\varphi_V + s\bar{s}\cos\varphi_V)\,\psi_\phi(s)\,,$$
$$\Psi_{f_0(980)}(s) = (n\bar{n}\cos\varphi + s\bar{s}\sin\varphi)\,\psi_{f_0(980)}(s)\,, \qquad (49)$$

assuming similar s-dependence for the $n\bar{n}$ and $s\bar{s}$ components. For $\psi_\phi(s)$ and $\psi_{f_0(980)}(s)$ the exponential parameterization is used, eq. (25). The radius squared of the $n\bar{n}$ component in the ϕ-meson is suggested to be approximately the same as that of the pion: $R^2_\phi(n\bar{n}) \simeq 10.9\,\mathrm{GeV}^{-2}$, while the radius squared for the $s\bar{s}$ component, $R^2_\phi(s\bar{s})$, appears to be slightly less, $R^2_\phi(s\bar{s}) \simeq 9.3\,\mathrm{GeV}^{-2}$, that corresponds to $b_\phi = 2.5\ \mathrm{GeV}^{-2}$. As to $f_0(980)$, we vary the radius of the $n\bar{n}$ component in the interval $6\,\mathrm{GeV}^{-2} \le R^2_{f_0(980)}(n\bar{n}) \le 18\,\mathrm{GeV}^{-2}$.

3.1.2 Partial width of $\phi(1020) \to \gamma f_0(980)$

The amplitude $A_{\phi\to\gamma f_0(980)}(0)$ is the sum of two terms related to the $n\bar{n}$ and $s\bar{s}$ components:

$$A_{\phi\to\gamma f_0}(0) = \cos\varphi\sin\varphi_V F^{(n\bar{n})}_{\phi\to\gamma f_0(980)}(0) + \sin\varphi\cos\varphi_V F^{(s\bar{s})}_{\phi\to\gamma f_0(980)}(0)\,. \qquad (50)$$

In our estimations we put $\cos\varphi_V \sim 0.99$ and, correspondingly, $|\sin\varphi_V| \sim 0.14$; for the $f_0(980)$ we vary the mixing angle in the interval $0^\circ \le |\varphi| \le 90^\circ$.

The results of the calculation are shown in figs. 3 and 4. In fig. 3a the values $A^{(n\bar{n})}_{\phi\to\gamma f_0(980)}(0)$ and $A^{(s\bar{s})}_{\phi\to\gamma f_0(980)}(0)$ are plotted *versus* radius squared, $R^2_{f_0(980)}$.

In fig. 4 one can see the value $\mathrm{BR}(\phi \to \gamma f_0(980))$ at various φ. Shaded areas correspond to the variation of φ_V in the interval $-8^\circ \le \varphi_V \le 8^\circ$; the lower and upper curves of the shaded area correspond to the destructive and constructive interferences of $A^{(n\bar{n})}_{\phi\to\gamma f_0(980)}(0)$ and $A^{(s\bar{s})}_{\phi\to\gamma f_0(980)}(0)$, respectively.

The measurement of the $f_0(980)$ signal in the $\gamma\pi^0\pi^0$ reaction (SND Collaboration) gives the branching ratio

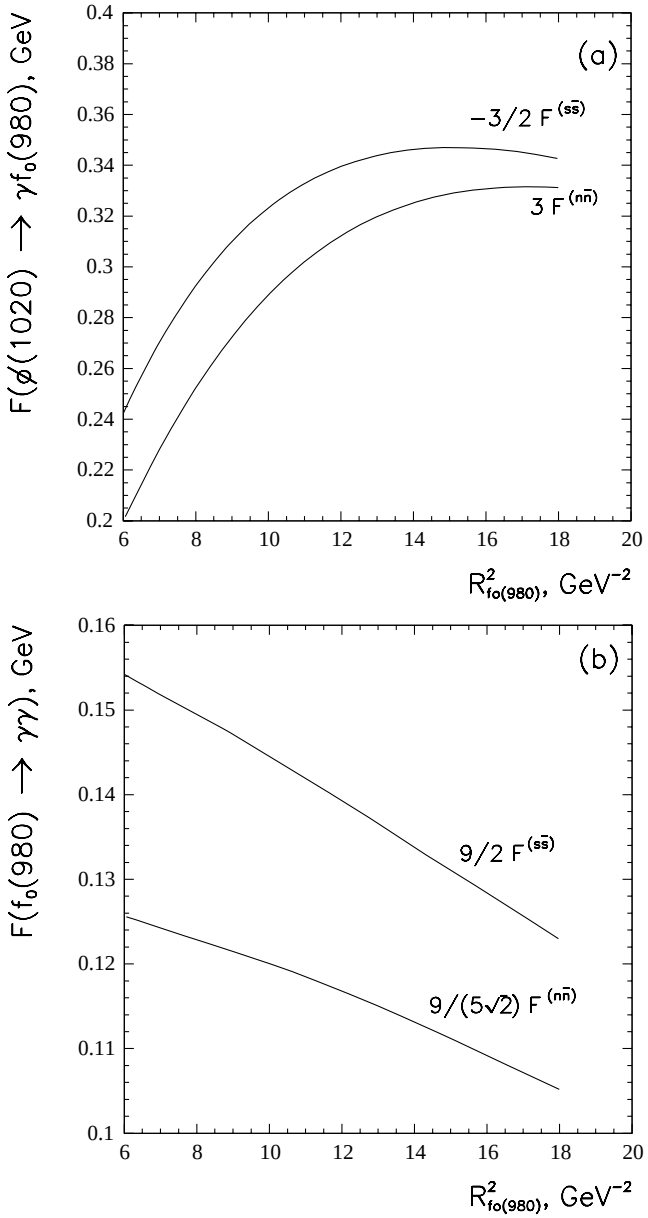

Fig. 3. Amplitudes for strange and nonstrange components, $s\bar{s}$ and $n\bar{n}$, as functions of the $f_0(980)$-meson radius squared: a) $F^{(n\bar{n})}_{\phi\to\gamma f_0}(0)/Z^{(n\bar{n})}_{\phi\to\gamma f_0}$ and $F^{(s\bar{s})}_{\phi\to\gamma f_0}(0)/Z^{(s\bar{s})}_{\phi\to\gamma f_0}$, b) $F^{(n\bar{n})}_{f_0\to\gamma\gamma}(0)/Z^{(n\bar{n})}_{f_0\to\gamma\gamma}$ and $F^{(s\bar{s})}_{f_0\to\gamma\gamma}(0)/Z^{(s\bar{s})}_{f_0\to\gamma\gamma}$.

$\mathrm{BR}(\phi \to \gamma f_0(980)) = (3.5 \pm 0.3^{+1.3}_{-0.5}) \times 10^{-4}$ [11]; in the analysis of $\gamma\pi^0\pi^0$ and $\gamma\pi^+\pi^-$ channels (CMD Collaboration) it was found $\mathrm{BR}(\phi \to \gamma f_0(980)) = (2.90 \pm 0.21 \pm 1.5) \times 10^{-4}$ [11]; the averaged value is given in [12]: $\mathrm{BR}(\phi \to \gamma f_0(980)) = (3.4 \pm 0.4) \times 10^{-4}$. In our estimation of the permissible interval for the mixing angle φ, we have used the averaged value given by [12], with the inclusion of systematic errors of the order of those found in [11]: $\mathrm{BR}(\phi \to \gamma f_0(980)) = (3.4 \pm 0.4^{+1.5}_{-0.5}) \times 10^{-4}$.

The calculated values of $\mathrm{BR}(\phi \to \gamma f_0(980))$ agree with experimental data for $|\varphi| \ge 25^\circ$; larger values of the mixing angle, $|\varphi| \ge 55^\circ$, correspond to a more compact struc-

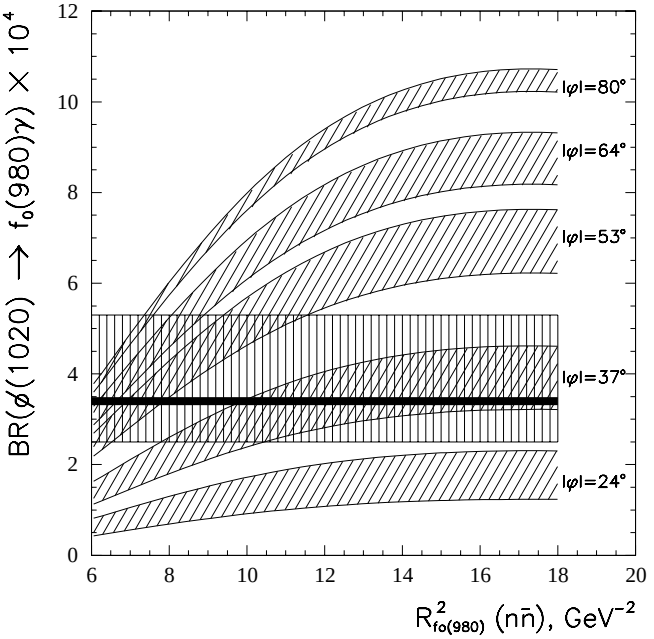

Fig. 4. Branching ratio $\mathrm{BR}(\phi(1020) \to \gamma f_0(980))$ as a function of radius squared of the $n\bar{n}$ component in $f_0(980)$. The band with vertical shading stands for the experimental magnitude: $\mathrm{BR}(\phi \to \gamma f_0(980)) = (3.4 \pm 0.4^{+1.5}_{-0.5}) \times 10^{-4}$. Five other bands, with skew shading, correspond to $|\varphi| = 24^\circ, 37^\circ, 53^\circ, 64^\circ, 80^\circ$ at $-8^\circ \le \varphi_V \le 8^\circ$.

ture of $f_0(980)$, namely, $R^2_{f_0(980)} \le 10\ \mathrm{GeV}^{-2}$, while small mixing angles, $|\varphi| \sim 25^\circ$, are related to a loosely bound structure of the $f_0(980)$, $R^2_{f_0(980)} \ge 12\ \mathrm{GeV}^{-2}$.

The evaluation of the radius of $f_0(980)$ was performed in [19] on the basis of GAMS data [20], where the t-dependence was measured in the process $\pi^- p \to f_0(980)\, n$ (t is the momentum squared transferred to $f_0(980)$): these data favour a comparatively compact structure of the $q\bar{q}$ component in $f_0(980)$, namely, $R^2_{f_0(980)} = 6 \pm 6\ \mathrm{GeV}^{-2}$.

3.2 Radiative decays $\phi(1020) \to \gamma\eta, \gamma\eta', \gamma\pi^0, \gamma a_0(980)$

The decays $\phi(1020) \to \gamma\eta, \gamma\eta'$ do not provide us with a direct information on the quark content of $f_0(980)$ and $\phi(1020)$; still, calculations and comparison with data are necessary to check the reliability of the method. The decays $\phi(1020) \to \gamma\pi^0$ and $\phi(1020) \to \gamma a_0(980)$ allow us to evaluate the admixture of the $n\bar{n}$ component in the ϕ-meson; as is seen in the previous section, this admixture affects significantly the value $\Gamma_{\phi(1020)\to\gamma f_0(980)}$.

For the transitions $\phi \to \gamma\eta$ and $\phi \to \gamma\eta'$ we take into account the dominant $s\bar{s}$ component only: $-\sin\theta\, s\bar{s}$ in η-meson and $\cos\theta\, s\bar{s}$ in η'-meson, with $\sin\theta = 0.6$.

For the pion wave function we have chosen $b_\pi = 2.0\ \mathrm{GeV}^{-2}$ that corresponds to $R^2_\pi = 10.1\ \mathrm{GeV}^{-2}$, the same radius is fixed for the $n\bar{n}$ component in η and η'. As to the strange component in η and η', we put its slope to be the same: $b_{\eta(s\bar{s})} = b_{\eta'(s\bar{s})} = 2\ \mathrm{GeV}^{-2}$, that leads to a smaller radius $R^2(s\bar{s}) = 8.3\ \mathrm{GeV}^{-2}$.

The calculation results for branching ratios compared to those given by the PDG compilation [12] are as follows:

$$\begin{aligned}
&\mathrm{BR}(\phi \to \eta\gamma) = 1.46 \times 10^{-2}\,,\\
&\mathrm{BR}_{\mathrm{PDG}}(\phi \to \eta\gamma) = (1.30 \pm 0.03) \times 10^{-2}\,,\\
&\mathrm{BR}(\phi \to \eta'\gamma) = 0.97 \times 10^{-4}\,,\\
&\mathrm{BR}_{\mathrm{PDG}}(\phi \to \eta'\gamma) = (0.67^{+0.35}_{-0.31}) \times 10^{-4}.
\end{aligned} \tag{51}$$

As is clearly seen, the calculated branching ratios agree reasonably with those given in [12].

For the process $\phi \to \gamma\pi^0$ the compilation [12] gives $\mathrm{BR}(\phi \to \gamma\pi^0) = (1.26 \pm 0.10) \times 10^{-3}$, and this value requires $|\sin\varphi_V| \simeq 0.07$ (or $|\varphi_V| \simeq 4^\circ$), for just with this admixture of the $n\bar{n}$ component in $\phi(1020)$ we reach the agreement with data. However, in the estimation of the allowed regions for mixing angle φ, fig. 4, we use

$$|\varphi_V| = 4^\circ \pm 4^\circ \tag{52}$$

considering the accuracy inherent to the quark model to be comparable with the obtained small value of $|\varphi_V|$.

The process $\phi(1020) \to \gamma a_0(980)$ depends also on the mixing angle $|\varphi_V|$: the decay amplitude is proportional to $\sin\varphi_V$, namely, $A_{\phi\to\gamma a_0} = \sin\varphi_V A^{(n\bar{n})}_{\phi\to\gamma a_0}$. For the region $R^2_{a_0(980)} \sim 8\ \mathrm{GeV}^{-2}$–$12\ \mathrm{GeV}^{-2}$, our calculation gives the following branching ratio:

$$\mathrm{BR}\,(\phi(1020) \to \gamma a_0(980)) = \sin^2\varphi_V \cdot (14 \pm 3) \times 10^{-4}\,, \tag{53}$$

with lower values for $R^2_{a_0(980)} \sim 8\ \mathrm{GeV}^{-2}$ and larger ones for $R^2_{a_0(980)} \sim 12\ \mathrm{GeV}^{-2}$. At $\sin^2\varphi_V = 0.01 \pm 0.01$, we have $\mathrm{BR}(\phi(1020) \to \gamma a_0(980)) = (0.14 \pm 0.14) \times 10^{-4}$.

In [11], the $\eta\pi^0$ spectrum was measured in the radiative decay $\phi(1020) \to \gamma\eta\pi^0$: it was found that $\mathrm{BR}(\phi(1020) \to \gamma\eta\pi^0;\ M_{\eta\pi} > 900\ \mathrm{MeV}) = (0.46 \pm 0.13) \times 10^{-4}$. This value does not contradict eq. (53) with $|\varphi_V| = 8^\circ$; moreover, if the ratio of the background/resonance in the region $M_{\eta\pi} \sim 900$ MeV is not small, that is rather possible, the value found in [11] agrees with smaller values of $|\varphi_V|$.

3.3 Radiative decays $f_0(980) \to \gamma\gamma$ and $a_0(980) \to \gamma\gamma$

The amplitude $A_{f_0(980)\to\gamma\gamma}(0,0)$ is determined by the contributions of two flavour components:

$$\begin{aligned}
A_{f_0(980)\to\gamma\gamma}(0,0) = {}& \cos\varphi F^{(n\bar{n})}_{f_0(980)\to\gamma\gamma}(0,0)\\
&+ \sin\varphi F^{(s\bar{s})}_{f_0(980)\to\gamma\gamma}(0,0)\,.
\end{aligned} \tag{54}$$

The amplitudes $A^{n\bar{n}}_{f_0(980)\to\gamma\gamma}(0,0)$ and $A^{s\bar{s}}_{f_0(980)\to\gamma\gamma}(0,0)$ depend on the radius squared of $f_0(980)$: these amplitudes plotted *versus* $R^2_{f_0(980)}$ are shown in fig. 3b.

Figure 5 demonstrates the comparison of the calculated partial width $\Gamma_{f_0(980)\to\gamma\gamma}$, at different $R^2_{f_0(980)}$ and φ, with the magnitude found in [15]: $\Gamma_{f_0(980)\to\gamma\gamma} =$

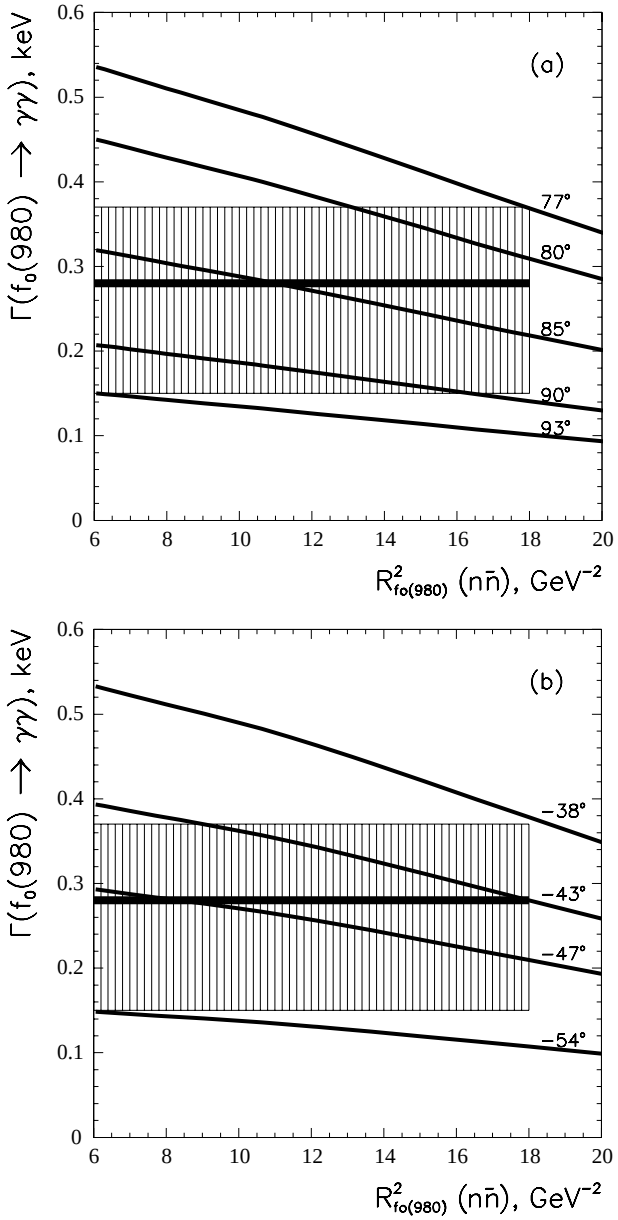

Fig. 5. Partial width $\Gamma_{f_0(980)\to\gamma\gamma}$; experimental data are from [15] (shaded area). Curves are calculated for a) positive mixing angles $\varphi = 77^\circ, 80^\circ, 85^\circ, 90^\circ, 93^\circ$ and b) negative mixing angles $\varphi = -38^\circ, -43^\circ, -47^\circ, -54^\circ$.

$0.28^{+0.09}_{-0.13}$. It is possible to describe the data using positive mixing angles $77^\circ \le \varphi \le 93^\circ$ as well as negative ones: $(-54^\circ) \le \varphi \le (-38^\circ)$.

The amplitude for the decay $a_0(980) \to \gamma\gamma$ is determined by the form factor of the $n\bar{n}$ component in the $f_0(980)$, with the only difference $\zeta_{f_0} \to \zeta_{a_0}$. The amplitude $A_{a_0(980)\to\gamma\gamma}/2\zeta_{a_0(980)\to\gamma\gamma}$ is shown in fig. 3b as a function of $R^2_{a_0(980)}$. Experimental study of $\Gamma(a_0(980) \to \gamma\gamma)$ was carried out in refs. [21,22], the averaged value is: $\Gamma(\eta\pi)\Gamma(\gamma\gamma)/\Gamma_{\rm total} = 0.24^{+0.08}_{-0.07}$ keV [12]. Using $\Gamma_{\rm total} \simeq \Gamma(\eta\pi) + \Gamma(K\bar{K})$, we have $\Gamma(a_0(980) \to \gamma\gamma) = 0.30^{+0.11}_{-0.10}$ keV. The calculated value of $\Gamma(a_0(980) \to \gamma\gamma)$ agrees with data at $R^2_{a_0(980)}$ belonging to the interval 10 GeV$^{-2} \le R^2_{a_0(980)} \le 26$ GeV^{-2}: the values of $R^2_{a_0(980)}$ of the order of $\sim$ 10–17 GeV^{-2} look quite reasonable for a meson of the $1^3P_0 q\bar{q}$ multiplet.

3.4 Partial widths for the two-photon decays of tensor mesons

Here we present our results for the decays $a_2(1320) \to \gamma\gamma$, $f_2(1270) \to \gamma\gamma$ and $f_2(1525) \to \gamma\gamma$.

3.4.1 Decay $a_2(1320) \to \gamma\gamma$

The form factor $F^{(H)}_{a_2(1320)\to\gamma\gamma}(0,0)$ is equal to that for the $n\bar{n}$ component, up to the charge factor:

$$F^{(H)}_{a_2(1320)\to\gamma\gamma}(0,0)/Z_{a_2(1320)} = F^{(H)}_{n\bar{n}\to\gamma\gamma}(0,0)/Z_{n\bar{n}}\,. \quad (55)$$

This universal form factor is determined by the spin structure of the vertex $a_2(1320) \to q\bar{q}$, which is regulated by the admixture of the ${}^3F_2 q\bar{q}$ state in $a_2(1320)$. Figure 6 shows the calculated form factor $F^{(H)}_{n\bar{n}\to\gamma\gamma}(0,0)/Z_{n\bar{n}}$ as a functions of R^2_T for different vertices given by eqs. (43), (45) and (46).

The comparison with data is performed for the form factors calculated with the use of minimal vertex given by eq. (43). In fig. 7 we plot calculated values of $\Gamma_{a_2(1320)\to\gamma\gamma}$ being a function of $R^2_{a_2(1320)}$ *versus* the data: $\Gamma_{a_2(1320)\to\gamma\gamma} = 0.98 \pm 0.05 \pm 0.09$ keV [23] and $\Gamma_{a_2(1320)\to\gamma\gamma} = 0.96 \pm 0.03 \pm 0.13$ keV [24]. The calculated value of $\Gamma_{a_2(1320)\to\gamma\gamma}$ reproduces data with $R^2_{a_2(1320)} \lesssim 9$ GeV^{-2} only. Still, one should not be convinced that larger values of the radius $R^2_{a_2(1320)}$ are excluded by the data. Experimental extraction of the signal $a_2(1320) \to \gamma\gamma$ faces the problem of a correct account for coherent background. This problem has been investigated in [25]: it was shown that the measured value of $\Gamma_{a_2(1320)\to\gamma\gamma}$ can fall down by a factor ~ 1.5, due to the interference "signal-background". Therefore, being careful, we estimate the region for $\Gamma_{a_2(1320)\to\gamma\gamma}$ allowed by the data as 1.12 keV$\le \Gamma_{a_2(1320)\to\gamma\gamma} \le 0.60$ keV.

Comparing the calculations with data, one should take into account uncertainties inherent in the model. In our calculation, $\Gamma_{a_2(1320)\to\gamma\gamma}$ strongly depends on the constituent quark mass. In fig. 6, the form factors and partial widths are depicted for $m_{u,d} = 350$ MeV and $m_s = 500$ MeV. However, decreasing of constituent quark mass by 10% results in the increase of the form factor $F^{(s)}_{n\bar{n}}(0,0)$ approximately by 10%, that means the 20% growth of the calculated value of $\Gamma_{a_2(1320)\to\gamma\gamma}$ at fixed $R^2_{a_2(1320)}$. The 10% uncertainty in the definition of the constituent quark mass looks quite reasonable, therefore, the 20% error in the model prediction for $\Gamma_{a_2(1320)\to\gamma\gamma}$ is to be regarded as normal.

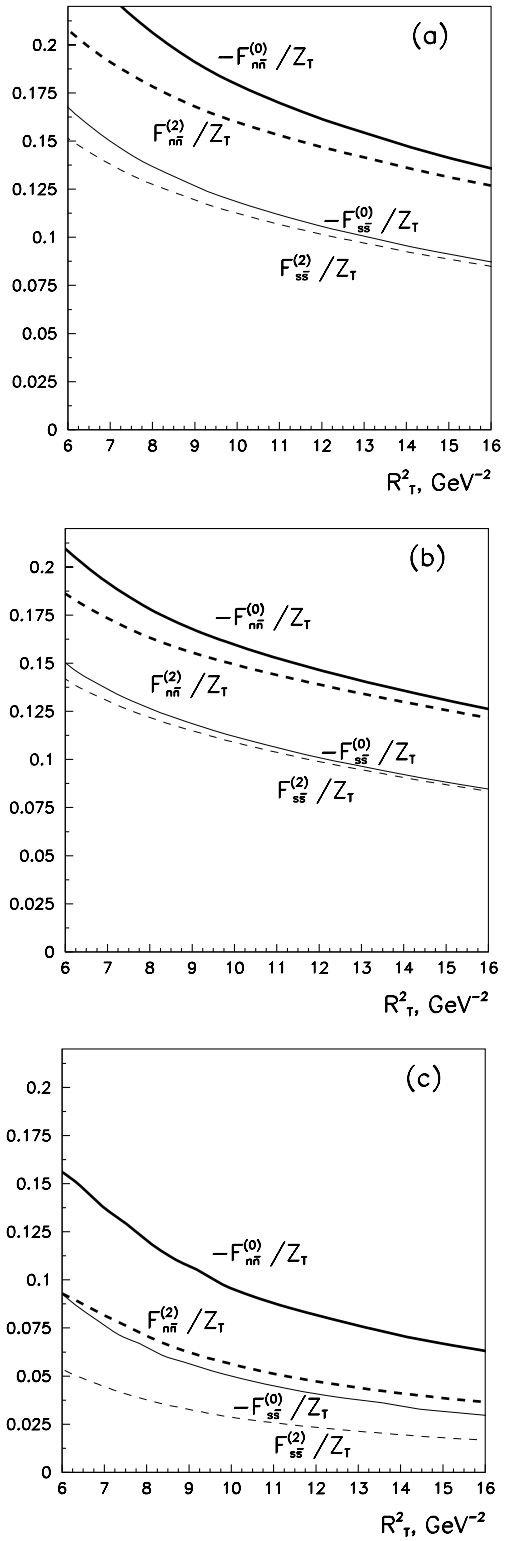

Fig. 6. Transition form factors $T \to \gamma\gamma$ (see (17) or (24)) for the nonstrange ($n\bar{n}$) and strange ($s\bar{s}$) quarks *versus* mean tensor-meson radius squared, R^2_T. a) $F^{(0)}_{q\bar{q}}(0,0)$ and $F^{(2)}_{q\bar{q}}(0,0)$ for $1^3P_2 q\bar{q}$ state with minimal vertex, eq. (41); b) the same as a) but with the vertex determined by (45); c) $F^{(0)}_{q\bar{q}}(0,0)$ and $F^{(2)}_{q\bar{q}}(0,0)$ for $1^3F_2 q\bar{q}$ state with vertex given by (46).

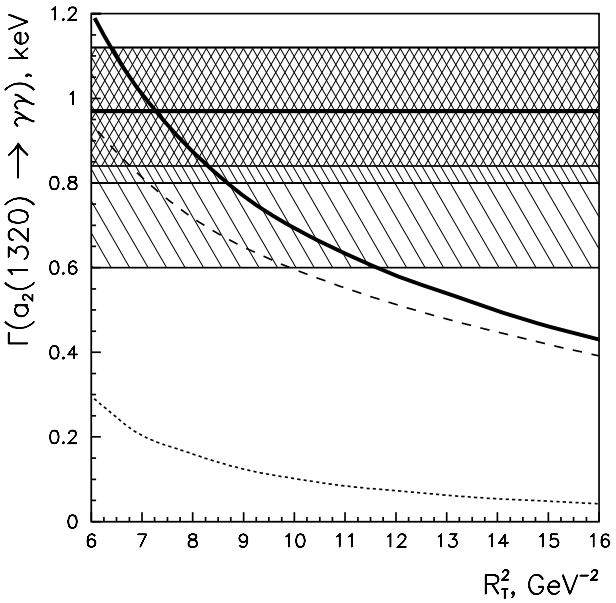

Fig. 7. Partial widths for $a_2 \to \gamma\gamma$ *versus* mean tensor-meson radius squared, R^2_T. Thick solid line: $\Gamma(a_2(1320) \to \gamma\gamma)$ for the vertex given by (43); dashed line: $\Gamma(a_2(1320) \to \gamma\gamma)$ for the vertex given by (45); dotted line: $\Gamma(a_2(\sim 2000) \to \gamma\gamma)$ for the vertex given by (46).

Summing up, the calculation of $\Gamma_{a_2(1320)\to\gamma\gamma}$ with the minimal vertex $a_2(1320) \to q\bar{q}$ given by (43) provides reasonable agreement with data at 7 GeV$^{-2} \lesssim R^2_{a_2(1320)} \lesssim$ 13 GeV^{-2}.

The vertex corresponding to the production of the $q\bar{q}$ pair in the F-wave, eq. (46), gives partial-width value $\sim$ 0.1 keV that is by an order of magnitude less than for the P-wave $q\bar{q}$ component.

The vertex for pure P-wave $q\bar{q}$ state, see (45), gives us a 10% smaller value of $\Gamma_{a_2(1320)\to\gamma\gamma}$ as compared to what is provided by minimal vertex (43).

3.4.2 The decays $f_2(1270) \to \gamma\gamma$ and $f_2(1525) \to \gamma\gamma$

We define the wave functions of $f_2(1270)$ and $f_2(1525)$ as follows:

$$\Psi_{f_2(1270)}(s) = (\cos\varphi_T\ n\bar{n} + \sin\varphi_T\ s\bar{s})\,\psi_T(s),$$
$$\Psi_{f_2(1525)}(s) = (-\sin\varphi_T\ n\bar{n} + \cos\varphi_T\ s\bar{s})\,\psi_T(s). \quad (56)$$

Then, the form factors for the two-photon decays of f_2-mesons read

$$F^{(H)}_{f_2(1270)\to\gamma\gamma}(0,0) = \cos\varphi_T F^{(H)}_{n\bar{n}\to\gamma\gamma}(0,0) + \sin\varphi_T F^{(H)}_{s\bar{s}\to\gamma\gamma}(0,0),$$
$$F^{(H)}_{f_2(1525)\to\gamma\gamma}(0,0) = -\sin\varphi_T F^{(H)}_{n\bar{n}\to\gamma\gamma}(0,0) + \cos\varphi_T F^{(H)}_{s\bar{s}\to\gamma\gamma}(0,0). \quad (57)$$

Following [12,23–25], we put the following values for partial widths: $\Gamma_{f_2(1270)\to\gamma\gamma} = (2.60 \pm 0.25^{+0.00}_{-0.25})$ keV and

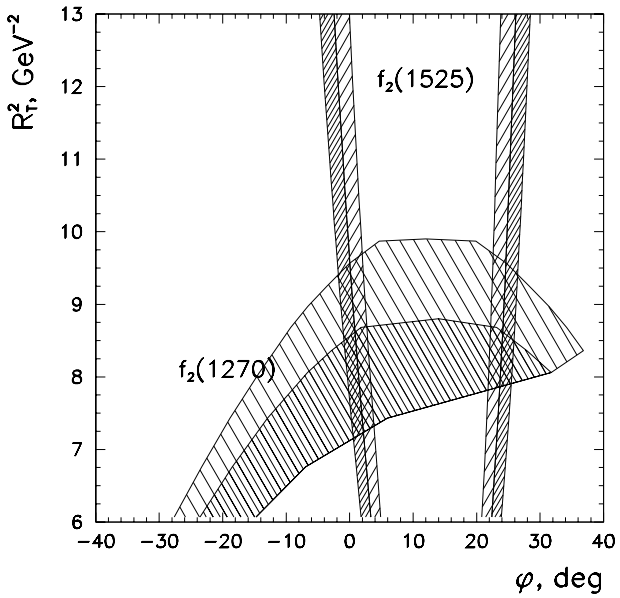

Fig. 8. The (R_T^2, φ)-plot, where φ is the mixing angle for the flavour components $f_2(1270) = n\bar{n}\cos\varphi + s\bar{s}\sin\varphi$ and $f_2(1525) = -n\bar{n}\sin\varphi + s\bar{s}\cos\varphi$; hatched areas show the regions allowed by data for the decays $f_2(1270) \to \gamma\gamma$ and $f_2(1525) \to \gamma\gamma$.

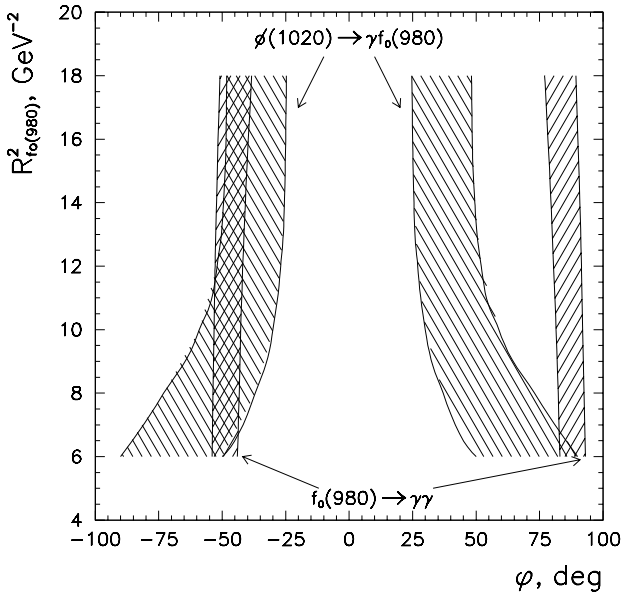

Fig. 9. The $(\varphi, R^2_{f_0(980)})$-plot: the shaded areas are the allowed regions for the reactions $\phi(1020) \to \gamma f_0(980)$ and $f_0(980) \to \gamma\gamma$.

$\Gamma_{f_2(1525)\to\gamma\gamma} = (0.097 \pm 0.015^{+0.00}_{-0.25})$ keV. The magnitude of the extracted signal depends on the type of model used for the description of the background. With coherent background, the magnitude of the signal decreases, and the second error in $\Gamma_{f_2(1270)\to\gamma\gamma}$ and $\Gamma_{f_2(1525)\to\gamma\gamma}$ is related to the background uncertainties.

A satisfactory description of the data has been reached with $R_T^2 \lesssim 10$ GeV^{-2} and two mixing angles φ_T: $\varphi_T \simeq 0°$ and $\varphi_T \simeq 25°$, see fig. 8. For example, at $R^2_{f_T} = 9$ GeV^{-2} and $\varphi_T = 0°$, the calculations result in $\Gamma_{f_2(1270)\to\gamma\gamma} = 2.240$ keV and $\Gamma_{f_2(1525)\to\gamma\gamma} = 0.090$ keV. Nearly the same values are reproduced at $R^2_{f_T} = 9$ GeV^{-2} and $\varphi_T = 25°$, namely, $\Gamma_{f_2(1270)\to\gamma\gamma} = 2.237$ keV and $\Gamma_{f_2(1525)\to\gamma\gamma} = 0.093$ keV.

As for the reaction $a_2(1320) \to \gamma\gamma$, the model uncertainties, $\sim$ 20%, are inherent in the calculations of $\Gamma_{f_2(1270)\to\gamma\gamma}$ and $\Gamma_{f_2(1525)\to\gamma\gamma}$.

4 Conclusion

Figure 9 demonstrates the $(\varphi, R^2_{f_0(980)})$-plot where the allowed areas for the reactions $\phi(1020) \to \gamma f_0(980)$ and $f_0(980) \to \gamma\gamma$ are shown. We see that radiative decays $\phi(1020) \to \gamma f_0(980)$ and $f_0(980) \to \gamma\gamma$ are well described in the framework of the hypothesis of the dominant $q\bar{q}$ structure of $f_0(980)$. The solution with negative φ seems more preferable. For this solution the mixing angle φ for the $n\bar{n}$ and $s\bar{s}$ components $(n\bar{n}\cos\varphi + s\bar{s}\sin\varphi)$ is equal to $\varphi = -48° \pm 6°$, that is, the $q\bar{q}$ component is rather close to the flavour octet ($\varphi_{\rm octet} = -54.7°$). However, the radiative-decay data do not exclude the variant when the $f_0(980)$ is an almost pure $s\bar{s}$ state with $\varphi = 85° \pm 5°$.

The dominance of the quark-antiquark component does not exclude the existence of other components in $f_0(980)$ on the level 10%–20%. The location of the resonance pole near the $K\bar{K}$ threshold definitely points to a certain admixture of the long-range $K\bar{K}$ component in $f_0(980)$. To investigate this admixture, precise measurements of the $K\bar{K}$ spectra in the interval 1000–1150 MeV are necessary: only these spectra could shed the light on the role of the long-range $K\bar{K}$ component in $f_0(980)$.

The existence of the long-range $K\bar{K}$ component or that of gluonium in the $f_0(980)$ results in a decrease of the $s\bar{s}$ fraction in the $q\bar{q}$ component: for example, if the long-range $K\bar{K}$ (or gluonium) admixture is of the order of 15%, the data require either $\varphi = -45° \pm 6°$ or $\varphi = 83° \pm 4°$.

There is no problem with the description of the decay $a_0(980) \to \gamma\gamma$ within the hypothesis about the $q\bar{q}$ origin of the $a_0(980)$: the data are in good agreement with the results of calculations at $R^2_{a_0(980)} \sim 10$–17 GeV^{-2}.

We have calculated the two-photon decays of tensor mesons, members of the $q\bar{q}$ multiplet $1^3P_2 q\bar{q}$. The calculated partial widths of radiative decays, $a_2(1320) \to \gamma\gamma$, $f_2(1270) \to \gamma\gamma$ and $f_2(1525) \to \gamma\gamma$, are in reasonable agreement with the data. The radial wave functions of $a_2(1320)$, $f_2(1270)$ and $f_2(1525)$ are close to those of $a_0(980)$ and $f_0(980)$ found in the study of the radiative decays $a_0(980) \to \gamma\gamma$, $f_0(980) \to \gamma\gamma$ and $\phi(1020) \to \gamma f_0(980)$. The possibility to simultaneously describe scalar and tensor mesons using approximately equal radial wave functions may be considered as a strong argument in favour of the fact that all these mesons, tensor ones, $a_2(1320)$, $f_2(1270)$ and $f_2(1525)$ and scalar ones, $a_0(980)$ and $f_0(980)$, are members of the same P-wave $q\bar{q}$ multiplet.

We are grateful to L.G. Dakhno, V.N. Markov, M.A. Matveev and A.V. Sarantsev for useful discussions. The paper is suppored by RFBR grant 01-02-17861.

References

1. R. Gatto, Phys. Lett. **17**, 124 (1965); V.V. Anisovich, A.A. Anselm, Ya.I. Azimov, G.S. Danilov, I.T. Dyatlov, Pis'ma Z. Eksp. Teor. Fiz. **2**, 109 (1965).
2. E. Klempt, *Meson spectroscopy: glueballs, hybrids, and q anti-q mesons*, hep-ex/0101031 (2001).
3. L. Montanet, Nucl. Phys. Proc. Suppl. **86**, 381 (2000).
4. R. Ricken, M. Koll, D. Merten, B.C. Metsch, H.R. Petry, Eur. Phys. J. A **9**, 221 (2000).
5. V.V. Anisovich, A.A. Anselm, Ya.I. Azimov, G.S. Danilov, I.T. Dyatlov, Phys. Lett. **16**, 194 (1965); W.E. Tirring, Phys. Lett. **16**, 335 (1965); L.D. Solovjev, Phys. Lett. **16**, 345 (1965); C. Becchi, G. Morpurgo, Phis. Rev. **140**, 687 (1965).
6. V.V. Anisovich, M.N. Kobrinsky, D.I. Melikhov, A.V. Sarantsev, Nucl. Phys. A **544**, 747 (1992).
7. V.V. Anisovich, D.I. Melikhov, V.A. Nikonov, Phys. Rev. D **52**, 5295 (1995).
8. V.V. Anisovich, D.I. Melikhov, V.A. Nikonov, Phys. Rev. D **55**, 2918 (1997).
9. A.V. Anisovich, V.V. Anisovich, D.V. Bugg, V.A. Nikonov, Phys. Lett. B **456**, 80 (1999).
10. D.I. Melikhov, Phys. Rev. D **56**, 7089 (1997); D.I. Melikhov, B. Stech, Phys. Rev. D **62**, 014006 (2000).
11. CMD-2 Collaboration (R.R. Akhmetshin *et al.*), Phys. Lett. B **462**, 371; 380 (1999); SND Collaboration (M.N. Achasov *et al.*), Phys. Lett. B **485**, 349 (2000).
12. PDG Group (D.E. Groom *et al.*), Eur. Phys. J. C **15**, 1 (2000).
13. V.V. Anisovich, D.V. Bugg, D.I. Melikhov, V.A. Nikonov, Phys. Lett. B **404**, 166 (1997).
14. A.V. Anisovich, V.V. Anisovich, Phys. Lett. B **467**, 289 (1999).
15. M. Boglione, M.R. Pennington, Eur. Phys. J. C **9**, 11 (1999).
16. PDG Group (C. Caso *et al.*), Eur. Phys. J. C **3**, 1 (1998).
17. A.V. Anisovich, V.V. Anisovich, V.N. Markov, M.A. Matveev, A.V. Sarantsev, *Moment operator expansion for the two-meson, two-photon and fermion-antifermion states*, hep-ph/0105330 (2001).
18. A.V. Anisovich, V.V. Anisovich, L. Montanet, V.A. Nikonov, Eur. Phys. J. A **6**, 247 (1999).
19. V.V. Anisovich, D.V. Bugg, A.V. Sarantsev, Phys. Lett. B **437**, 209 (1998); Phys. At. Nucl. **62** , 289 (1999).
20. Yu.D. Prokoshkin *et al.*, Fiz. Dokl. **342**, 473 (1995); D. Alde *et al.*, Z. Phys. C **66**, 375 (1995).
21. JADE Collaboration (T. Oest *et al.*), Z. Phys. C **47**, 343 (1990).
22. Crystal Ball Collaboration (D. Antreasyan *et al.*), Phys. Rev. D **33**, 1847 (1986).
23. L3 Collaboration (M. Acciarri *et al.*), Phys. Lett. B **413**, 147 (1997).
24. ARGUS Collaboration (H. Albrecht *et al.*), Z. Phys. C **74**, 469 (1997).
25. ARGUS Collaboration (H. Albrecht *et al.*), Z. Phys. C **48**, 183 (1990).